2021 NDIA GROUND VEHICLE SYSTEMS ENGINEERING AND TECHNOLOGY SYMPOSIUM
MODELING, SIMULATION AND SOFTWARE (MS2) TECHNICAL SESSION
AUGUST 10-12, 2021 - NOVI, MICHIGAN

PHYSICS BASED SINGLE-WHEEL MODULE SLIPPAGE ASSESSMENT FOR AUTONOMOUS CONTROL DESIGN

Masood Ghasemi, PhD[1], Vladimir Vantsevich, PhD[1], David Gorsich, PhD[2], Jill Goryca[2], Amandeep Singh, PhD[2], Lee Moradi, PhD[1]

[1]The University of Alabama at Birmingham, Birmingham, AL
[2]U.S. Army Ground Vehicle Systems Center, Warren, MI

ABSTRACT

In this paper, a conceptually new research direction of the tire slippage analysis is provided as a new technological paradigm for agile tire slippage control. Specifically, the friction coefficient-slippage dynamics is analyzed and its characteristic parameters are introduced. Next, the nonlinear relation between the wheel torque and the tire instantaneous rolling radius incorporating the longitudinal elasticity factor is analyzed. The relation is shown to be related to the tire slippage. Further, its importance is clarified by deriving its dynamics and specifically, the instruction is given how it can be utilized to control slippage. Finally, the indices are introduced to assess the mobility and agility of the wheel in order to achieve optimal response to severe terrain conditions. The indices comprise of the introduced friction coefficient-slippage characteristic parameters.

Citation: M. Ghasemi, V. Vantsevich, D. Gorsich, J. Goryca, A. Singh, L. Moradi, "Physics Based Single-Wheel Module Slippage Assessment for Autonomous Control Design", In *Proceedings of the Ground Vehicle Systems Engineering and Technology Symposium* (GVSETS), NDIA, Novi, MI, Aug. 10-12, 2021.

1. INTRODUCTION

A critical problem in wheel dynamics is to establish the relationship between the tire kinematics and force characteristics related to tire slippage and thus, to estimate and control wheel mobility and tire-soil power losses. Over the past decades, parameters and characteristics of the vehicle-tire-terrain interaction have been thoroughly identified and characterized in numerous terramechanics and vehicle dynamics studies [1-3]. However, technical advantages that autonomy features can bring to dynamics and mobility of terrain vehicles urge the need to review and rethink the current fundamentals of tire slippage. Consequently, it is required to introduce a more advanced characterization of tire slippage for use in autonomous mobility control, particularly in severe terrain conditions.

The mobility control features are directly impacted by the tire slippage behavior characterized based on its temporal variations, spatial dynamics, and boundaries. Such features appear in different slippage control approaches reported in the literature including proportional-integral (PI) control [4, 5], variable structure PI (VSPI) control [4, 5], linear quadratic regulator

(LQR) [6], sliding mode control (SMC) [4, 5, 7], model predictive control (MPC) [8]. The underlying basis for these approaches is in utilizing the tire slippage dynamics given its boundaries that is the maximum allowed slippage amplitude.

Nonetheless, vehicle mobility and slippage highly depend on the terrain and tire attributes and their interaction dynamics. Specifically, in off-road applications, they are characterized by high level of uncertainties due to stochastic conditions, unevenness, deformability, material, grain size, and moisture content associated with the terrain. Thus, it is deemed critical for a robust and agile vehicle mobility control to establish a unified analysis trend to characterize tire-soil interaction and slippage dynamics and attributes. In this regard, a conceptually new research direction of the tire slippage analysis is presented as a new technological paradigm for agile tire slippage control, which targets extremely fast, precise and pre-emptive estimation and control solutions with response time less than the tire relaxation time [9, 10].

2. VEHICLE AGILITY

Agility is an important aspect of vehicles, particularly combat vehicles of all kinds. For aerial vehicles, flight agility is defined as the ability to rapidly transition from one state to another [11]. For ground vehicles, agility is phrased or referred to different aspects of vehicle dynamic behavior such as maneuvering, jerking, survivability, or cornering performance, which may depend on design balance, terrain, weather and a specified mission profile [12-14]. More discussion can be found in [14].

In this paper, however, agility in autonomous vehicle control relates to performance that the vehicle is expected to demonstrate in much more severe terrain conditions than conventional vehicles with operators. Specifically, it is thought of as a very fast (hyper dynamic), precise, and continuously reproduced response of decision making and control systems to provide and maintain required autonomous vehicle performance in the presence of unexpected man-made and uncertain terrain.

The underlying dynamical attribute that determines the agility performance of a vehicle is its response time of traction/mobility control systems to a change of tire gripping conditions. There are three distinct dynamical features/sub-systems affecting a control system's response time and thus, its agility performance: 1) the plant, which comprises the physical system, 2) the sensory data acquisition and estimation processes, and 3) the actuation and control processes. Due to interconnection of these dynamical sub-systems, the closed-loop system's response time is a function of the summation of the lags induced by each of these sub-systems. Therefore, the vehicle agility infers the agility of all its sub-systems.

The response time of current control systems is over 100 to 120 milliseconds, which is higher than the tire relaxation time ranging from 40 to 80 milliseconds [15]. Thus, the wheels already spin before the traction control engages and vehicle mobility is lost. Further improvements of terrain mobility of vehicles can be achieved by reducing the response time of the control systems. Thus, development of such control systems requires a comprehensive rethinking of the tire slippage dynamics and its inherent coupling with forward linear and rotational dynamics as well as normal dynamics of the wheel itself.

An enabling technology to address the above problem is electric drivetrains, and in particular of in-wheel-motor (IWM) [16, 17], which enhances the potential for agile mobility control and maneuverability and energy efficiency optimization of vehicles. The underlying potentials are three-fold: 1) a faster response and higher bandwidth due to electric motor dynamics characteristics and a compact mechanical driveline for power delivery, 2) a more precise torque modulation, and 3) coordinated control of all individual wheels [4, 8, 18]. The next section discusses the dynamics of a system comprising the IWM technology.

3. DYNAMICS OF A SINGLE-WHEEL MODULE (SWM)

This paper presents an analysis of the tire slippage process in stochastic terrain conditions and develops a set of tire-soil characteristics for modeling, estimation and control of agile tire slippage. To illustrate the results a single-wheel module (SWM) is being utilized. The SWM is a simulation model of a quarter of a 4x4 vehicle including a single wheel-tire system, propulsion system (electric motor and driveline), brake, suspension, and steering. Further, it is equipped with an IWM technology, which unlike conventional drivelines, it offers a compact mechanical path for power delivery. Such a mechanical design in combination with a fast electrical motor with a response time in the range of a few milliseconds, satisfies the physical system's agility requirements.

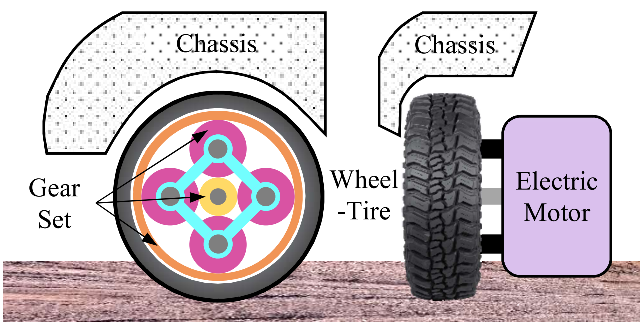

Figure 1. The propulsion system of the SWM.

Figure 1 illustrates the schematic of the propulsion system of the SWM. This sub-system is powered by an electric motor whose generated power is transmitted through a reduction gear set to the wheel, and thus, drives the SWM forward.

The rotational dynamics of the wheel is given as

$$\dot{\omega}_{\mathrm{w}}(t) = \frac{1}{J_{\mathrm{eq}}}\left(T_{\mathrm{w}}(t) - T_{\mathrm{wl}}(t)\right), \tag{1}$$

where $T_{\mathrm{w}}(\cdot): \mathbb{R} \to \mathbb{R}$ is the wheel torque, $T_{\mathrm{wl}}(\cdot): \mathbb{R} \to \mathbb{R}$ is the wheel load torque, rolling resistance, J_{eq} is the equivalent rotational inertia of the rotating components of the SWM (including the rotor shaft, the gears and the wheel) calculated at the wheel side.

The longitudinal dynamics is given as

$$\dot{v}_x = \frac{1}{M}(F_x(t) - R_x(t)), \tag{2}$$

where $v_x \in \mathbb{R}$ is the wheel linear speed, $F_x(\cdot): \mathbb{R} \to \mathbb{R}$ is the circumferential reaction force, $R_x(\cdot): \mathbb{R} \to \mathbb{R}$ is the resistance to motion force including the rolling resistance, the drag force, the drawbar force, and the resistance due to road slope (defined as $(m_{\mathrm{s}} + m_{\mathrm{u}})g\sin\theta$, where m_{s} and m_{u} are the sprung and unsprung masses, respectively, g is the gravity acceleration, and $\theta \in \mathbb{R}$ is the slope of the road), and $M \triangleq m_{\mathrm{s}} + m_{\mathrm{u}}$.

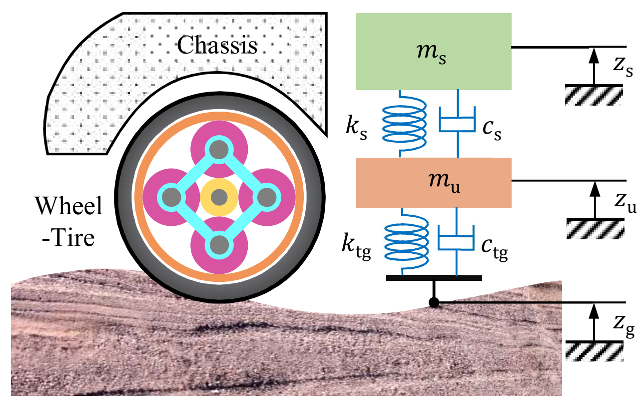

Figure 2. The sprung-unsprung mass system of the SWM.

The dynamics of the sprung-unsprung mass system (Figure 2) is given as

$$\ddot{z}_{\mathrm{s}}(t) = \frac{c_{\mathrm{s}}}{m_{\mathrm{s}}}\left(\dot{z}_{\mathrm{u}}(t) - \dot{z}_{\mathrm{s}}(t)\right) + \frac{k_{\mathrm{s}}}{m_{\mathrm{s}}}\left(z_{\mathrm{u}}(t) - z_{\mathrm{s}}(t)\right), \tag{3}$$

$$\ddot{z}_{\mathrm{u}}(t) = \frac{c_{\mathrm{s}}}{m_{\mathrm{u}}}\left(\dot{z}_{\mathrm{s}}(t) - \dot{z}_{\mathrm{u}}(t)\right) + \frac{k_{\mathrm{s}}}{m_{\mathrm{u}}}\left(z_{\mathrm{s}}(t) - z_{\mathrm{u}}(t)\right) + \frac{c_{\mathrm{tg}}}{m_{\mathrm{u}}}\left(\dot{z}_{\mathrm{g}}(t) - \dot{z}_{\mathrm{u}}(t)\right) + \frac{k_{\mathrm{tg}}}{m_{\mathrm{u}}}\left(z_{\mathrm{g}}(t) - z_{\mathrm{u}}(t)\right), \tag{4}$$

where $z_{\mathrm{s}}, z_{\mathrm{u}} \in \mathbb{R}$ are the vertical displacement of the sprung mass and unsprung mass, respectively, $z_{\mathrm{g}} \in \mathbb{R}$ is the terrain height with respect to a global reference, $k_{\mathrm{s}}, c_{\mathrm{s}}$ are the stiffness and damping coefficient of the sprung mass, $k_{\mathrm{tg}}, c_{\mathrm{tg}}$ are the equivalent stiffness and damping coefficient of the tire-ground.

Note that the rotational dynamics is coupled with the longitudinal dynamics as well as the normal dynamics of the sprung-unsprung sub-system dynamics through the tire-terrain interaction. The relations are given as

$$T_{\mathrm{wl}}(t) = r_{\mathrm{w}}^{0} F_x(t) = r_{\mathrm{w}}^{0} \mu_x R_z(t), \tag{5}$$

$$R_z(t) = (m_{\mathrm{s}} + m_{\mathrm{u}}) g \cos\theta(t) + c_{\mathrm{tg}} \left(\dot{z}_{\mathrm{g}}(t) - \dot{z}_{\mathrm{u}}(t) \right) + k_{\mathrm{tg}} \left(z_{\mathrm{g}}(t) - z_{\mathrm{u}}(t) \right), \tag{6}$$

where $F_x(\cdot): \mathbb{R} \to \mathbb{R}$ is the circumferential force, $R_z(\cdot): \mathbb{R} \to \mathbb{R}$ is the normal reaction force, r_{w}^{0} is the rolling radius of the tire in driven mode calculated for zero wheel torque, and $\mu_x \in (0,1)$ is the current friction coefficient, which is the normalized circumferential force that generally depends on the tire-terrain attributes and is functionally linked to the tire slippage. The tire slippage or slip ratio is a non-dimensional measure of the difference of the wheel actual linear speed, v_x, and its theoretical linear speed at zero slippage, $v_{\mathrm{t}}(t) \triangleq r_{\mathrm{w}}^{0} \omega_{\mathrm{w}}(t)$. The slippage definition is given as

$$s_\delta(t) = 1 - \frac{v_x(t)}{r_{\mathrm{w}}^{0} \omega_{\mathrm{w}}(t)}. \tag{7}$$

The current friction coefficient model for off-road application defined in [3] is given as

$$\mu_x(t) = \mu_{\mathrm{px}} \left(1 - \exp\left(-k s_\delta(t) \right) \right), \tag{8}$$

where $\mu_{\mathrm{px}} \in (0,1)$ is the peak friction coefficient, and $k > 0$ is an empirical factor that depends on the tire and terrain properties. Figure 3 depicts such a relation for different values of the peak friction coefficient and the parameter k.

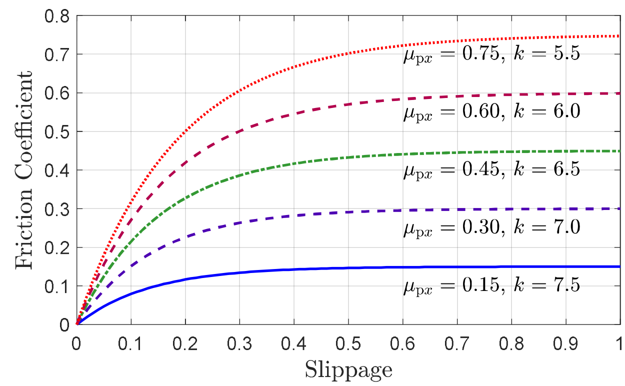

Figure 3. The typical relation between the friction coefficient and the slippage in off-road terrains.

4. SLIPPAGE DYNAMICS

The tire slippage is a function of the wheel linear and angular speeds. The variation of the slippage with respect to time is given as

$$\dot{s}_\delta(t) = \frac{\dot{\omega}_{\mathrm{w}}(t) v_x(t) - \omega_{\mathrm{w}}(t) \dot{v}_x(t)}{r_{\mathrm{w}}^{0} \omega_{\mathrm{w}}^{2}(t)}, \tag{9}$$

where $\dot{\omega}_{\mathrm{w}}(t)$ and $\dot{v}_x(t)$ are given by equations (1) and (2), respectively. Equation (7) indicates that the slippage variation is a function of the forward linear and rotational dynamics, which are coupled through tire-soil interaction and essentially due to the traction force. The slippage rate can indicate if the wheel is about to spin and loose traction or is already spinning and lost traction. At this critical condition, the slippage rate is increasing very fast. This analysis incorporates rate of two key variables utilized to assess the slippage behavior: the slippage and the friction coefficient, which are related as

$$\frac{d\mu_x(t)}{ds_\delta(t)} = \frac{\dot{\mu}_x(t)}{\dot{s}_\delta(t)}. \tag{10}$$

The importance of equation (10) is with the fact that it correlates the friction coefficient-slippage space to the dynamics of the wheel. Further, the instantaneous time derivatives can be estimated by which a direct analysis of the slippage characteristics is possible. Considering the traction force-slippage relation, the critical condition is defined as the area of the peak traction force, or when the rate of changes of the traction force is close to zero that is $\dot{F}_x(t) \approx 0$. Considering this definition, the slippage dynamics at the critical condition is obtained. Assuming that the resisting forces acting on the wheel is quasi-stationary, it is concluded from equation (2) that $\dot{v}_x(t) \approx 0$. Thus equation (9) yields

$$\dot{s}_\delta(t) = \frac{\dot{\omega}_\mathrm{w}(t) v_x(t)}{r_\mathrm{w}^0 \omega_\mathrm{w}^2(t)}. \quad (11)$$

Rewriting equation (11) gives

$$\frac{\dot{s}_\delta(t)}{\dot{\omega}_\mathrm{w}(t)} = \frac{ds_\delta(t)}{d\omega_\mathrm{w}(t)} \approx \frac{v_x(t)}{r_\mathrm{w}^0 \omega_\mathrm{w}^2(t)}. \quad (12)$$

Note that $v_x(t) = v_x$ is almost constant at the critical situation. Thus,

$$\frac{ds_\delta(t)}{d\omega_\mathrm{w}(t)} \approx \frac{\kappa}{\omega_\mathrm{w}^2(t)}, \quad (13)$$

where $\kappa \triangleq v_x / r_\mathrm{w}^0$ is almost constant. Integrating equation (13) gives

$$s_\delta(t) = 1 - \frac{\kappa}{\omega_\mathrm{w}(t)}. \quad (14)$$

Equation (14) indicates that during the mobility critical conditions, the wheel angular speed increases very fast with the growth of slippage. This behavior is illustrated in Figure 4. The plots are associated with those in Figure 3.

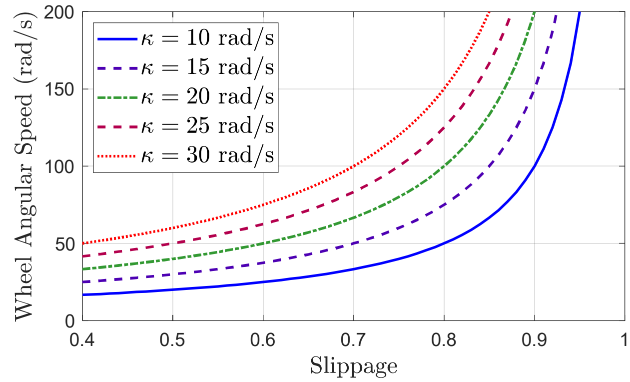

Figure 4. The effect of the slippage growth on the wheel angular speed at the mobility critical condition.

4.1. CHARACTERISTIC SLIPPAGE

It is essential for mobility control to know when the systems enters the critical mobility condition as illustrated in Figure 4. The onset of the critical mobility condition is identified by the characteristic slippage defined as a slippage after which the traction-slippage characteristic becomes quasi-linear. The nonlinearity of a continuous function can be identified by non-zero higher order derivatives (orders more than one), which contribute to nonlinear terms in its Taylor expansion. The second derivative of equation (8) gives

$$\nu(s_\delta) \triangleq \frac{d^2\mu_x(t)}{ds_\delta^2(t)} = -k^2 \mu_{\mathrm{px}} \exp\left(-k s_\delta(t)\right), \quad (15)$$

where ν is the curvature of friction coefficient-slippage diagram. The characteristic slippage, $s_{\delta\mathrm{c}}$, is associated with a characteristic curvature after which the behavior of the traction-slippage is quasi-linear. Let $\nu(s_{\delta\mathrm{c}}) = \nu_\mathrm{c}$. Then, the characteristic slippage is obtained as

$$s_{\delta\mathrm{c}} = \frac{1}{k} \mathrm{Ln} \frac{k^2 \mu_{\mathrm{px}}}{-\nu_\mathrm{c}}. \quad (16)$$

Note that the characteristic curvature, ν_c, is a mathematical parameter, which is related to the friction coefficient-slippage curve comprising normalized non-dimensional variables. Thus, a single value can be chosen for ν_{c} addressing all different friction coefficient-slippage curves.

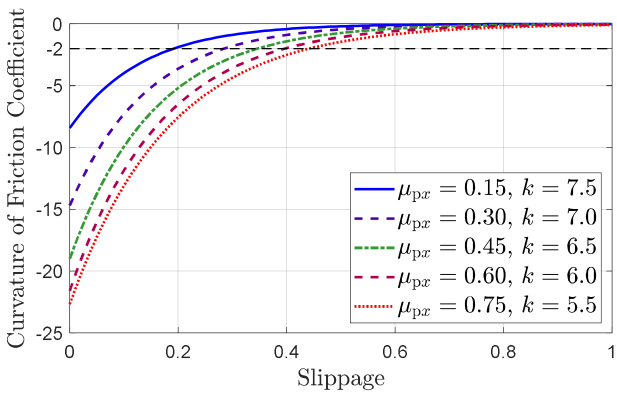

Figure 5. The curvature of the friction coefficient as an indicator of the slippage behavior.

The curvature of friction coefficient-slippage of equation (8) is illustrated in Figure 5. The plots are associated with those in Figure 3. The horizontal dashed line is with the characteristic curvature ($\nu_{\mathrm{c}} = -2$), which roughly separates the nonlinear and quasi-linear sections. The intersections of the horizontal line and the curves determine their respective characteristic slippages. For instance, the characteristic slippage for the blue curve is about 20%, while it is about 45% for the dotted red curve.

Substituting the characteristic slippage of equation (16) into equation (8) yields

$$\mu_{xc} = \mu_{\mathrm{px}}\left(1 + \frac{\nu_{\mathrm{c}}}{k^2\mu_{\mathrm{px}}}\right) = \mu_{\mathrm{px}} + \frac{\nu_{\mathrm{c}}}{k^2}. \quad (17)$$

where μ_{xc} is the characteristic friction coefficient, which indicates the maximum friction coefficient the wheel can reach before it loses mobility. Note that $\mu_{xc} < \mu_{\mathrm{px}}$, since the characteristic curvature is negative.

5. TIRE INSTANTANEOUS ROLLING RADIUS

The instantaneous rolling radius intrinsically depends on the wheel torque. The relation is nonlinear in general and can be expressed as

$$r_{\mathrm{w}}(t) = f\big(T_{\mathrm{w}}(t)\big), \quad (18)$$

where $f(\cdot): \mathbb{R} \to \mathbb{R}$. One form of $f(\cdot)$ is given as [3]

$$r_{\mathrm{w}}(t) = r_{\mathrm{w}}^0 - \lambda_{\mathrm{w}}(t)T_{\mathrm{w}}(t), \quad (19)$$

where $\lambda_{\mathrm{w}}(\cdot): \mathbb{R} \to \mathbb{R}$ is the longitudinal elasticity factor of a tire on the road or the combined elasticity factor of a tire and soil in off-road terrain. The above relation is illustrated in Figure 6.

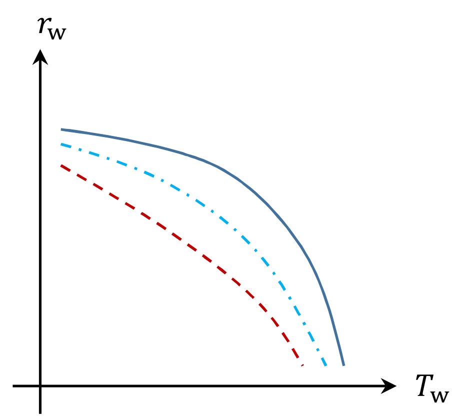

Figure 6. The general nonlinear relation between the instantaneous tire rolling radius and the wheel torque.

Rewriting equation (19) gives

$$\lambda_{\mathrm{w}}(t) = \frac{r_{\mathrm{w}}^0 - r_{\mathrm{w}}(t)}{T_{\mathrm{w}}(t)} = \frac{r_{\mathrm{w}}^0 s_\delta(t)}{T_{\mathrm{w}}(t)}. \quad (20)$$

Note that $\lambda_{\mathrm{w}}(t) \geq 0$ since $T_{\mathrm{w}}(t)s_\delta(t) \geq 0$. If the longitudinal elasticity factor is given, then the dynamical relation of the tire slippage and the wheel torque is known. The dynamics of the tire longitudinal elasticity factor is obtained by differentiating equation (20) with respect to time. Specifically, one can get

$$r_w^0 \dot{s}_\delta(t) = \lambda_\mathrm{w}(t)\dot{T}_\mathrm{w}(t) + T_\mathrm{w}(t)\dot{\lambda}_\mathrm{w}(t) \qquad (21)$$

The importance of equations (20)-(21) is that they are keys to the slippage control design. Specifically, from a control design perspective, it is desirable to know how the wheel torque should be adjusted in order for the instantaneous rolling radius and thus, the slippage to have a specific dynamical behavior. For instance, during acceleration or braking, the magnitude of the slippage should be the maximum allowed, that is the characteristic slippage. For a general case of slippage control, one can define the slippage tracking error as $e_s(t) \triangleq s_\delta(t) - s_{\delta\mathrm{r}}(t)$, where $s_{\delta\mathrm{r}}(\cdot)$ is the reference slippage. Next consider a stable profile given by

$$\dot{e}_s(t) + Ke_s(t) = 0 \qquad (22)$$

where $K > 0$ is the proportional control gain. Substituting slippage and its time derivative from equations (20)-(21) into equation (22) yields

$$\begin{aligned}\lambda_\mathrm{w}(t)\dot{T}_\mathrm{w}(t) = &-\dot{\lambda}_\mathrm{w}(t)T_\mathrm{w}(t) - K\lambda_\mathrm{w}(t)T_\mathrm{w}(t)\\ &+r_\mathrm{w}^0(\dot{s}_{\delta\mathrm{r}}(t) + Ks_{\delta\mathrm{r}}(t))\end{aligned} \qquad (23)$$

The wheel torque is considered as a reference torque for the lower level control at the electric motor side. Further, note that the wheel torque is proportional to the electric current of the electric motor (in either AC or DC type) assuming that the flexibility of the mechanical connection between the motor and the wheel is negligible. Thus, equation (23) can be expanded to obtain a control solution as $\dot{T}_\mathrm{w}(t)$ is inherently a function of the control input at the electric motor side.

6. MOBILITY

An on-line vehicle dynamics-based mobility estimation method is proposed in [19, 20]. Specifically, the method is based on the wheel mobility index (WMI) given as [19, 20]

$$\mathfrak{M}_\mathrm{w}(t) = 1 - \frac{\mu_x(t)}{\mu_{\mathrm{p}x}} \qquad (24)$$

Equation (24) linearly relates the current friction coefficient to the wheel mobility and in particular, it states that if the current friction coefficient is equal to the peak friction coefficient, the mobility is zero. However, it is desired that the friction coefficient stays below its characteristic value. In order to incorporate the characteristic friction coefficient in the definition, a modified WMI is introduced given as

$$\widetilde{\mathfrak{M}}_\mathrm{w}(t) = \begin{cases} 1 - \frac{\mu_x(t)}{\mu_{x\mathrm{c}}}, & s_\delta(t) \le s_{\delta\mathrm{c}} \\ 0, & s_\delta(t) > s_{\delta\mathrm{c}} \end{cases}. \qquad (25)$$

Further, the combined wheel mobility-agility index (WMAI) is introduced by incorporating the friction coefficient into WMI or its modified variation. Specifically, the WMAI based on equation (24) is given as

$$\mathfrak{M}_\mathrm{aw}(t) = \mu_x(t)\left(1 - \frac{\mu_x(t)}{\mu_{\mathrm{p}x}}\right), \qquad (26)$$

Alternatively, the WMAI based on equation (25) is given as

$$\widetilde{\mathfrak{M}}_\mathrm{aw}(t) = \begin{cases} \mu_x(t)\left(1 - \frac{\mu_x(t)}{\mu_{x\mathrm{c}}}\right), & s_\delta(t) \le s_{\delta\mathrm{c}} \\ 0, & s_\delta(t) > s_{\delta\mathrm{c}} \end{cases}. \qquad (27)$$

The WMAI determines the optimal ranges of tire slippage where the mobility is good while the traction is sufficient for agile response to severe terrain conditions such as a transition to low friction terrain. The relations are illustrated in Figure 8 and Figure 8 for different friction coefficient-slippage diagrams of Figure 5.

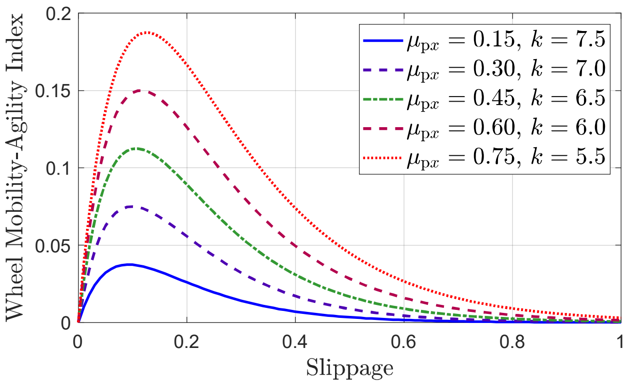

Figure 7. Illustration of the WMAI for different friction coefficient attributes based on the WMI.

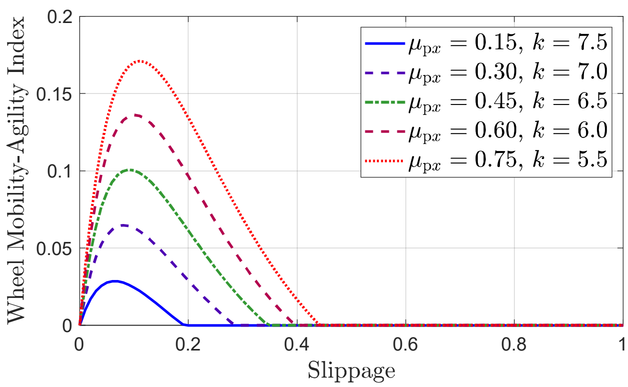

Figure 8. Illustration of the WMAI for different friction coefficient attributes based on the modified WMI.

The WMAI and the modified WMAI indicate almost similar optimal slippage regions for a single wheel dynamics. Nonetheless, the modified WMAI imposes boundary conditions on the optimal solution that is the slippage must be less than its characteristic value. This is particularly important when a mobility optimization problem for a vehicle is considered. Each wheel of a vehicle might exhibit different dynamic attributes due to different tire-terrain dynamics, steering, curvilinear motion, and side slip. Thus, the overall optimal solution may lead to a wheel operate with high slippage. The utilization of the modified WMAI for optimal problem for a vehicle facilitates direct implementation of the boundary conditions and ensures that the slippages of all wheels are maintained below their characteristic values.

7. CONCLUSION

In this paper, a conceptually new research direction of the tire slippage analysis was provided as a new technological paradigm for agile tire slippage control. The analysis focused on how the friction coefficient-slippage attributes and dynamics can contribute to wheel mobility and agile control. A similar analysis was performed for the wheel torque utilizing its relation with the tire instantaneous rolling radius and thus, tire slippage. Finally, the indices were introduced to assess the mobility and agility of the wheel dynamics in order to achieve optimal response to severe terrain conditions. The indices comprise of the introduced friction coefficient-slippage characteristic parameters. The results will be used in another research work to design agile control system for a SWM.

REFERENCES

[1] J. Y. Wong, *Theory of ground vehicles*, 4 ed.: John Wiley & Sons, 2008.

[2] J. Y. Wong, P. Jayakumar, E. Toma, and J. Preston-Thomas, "A review of mobility metrics for next generation vehicle mobility models," *Journal of Terramechanics,* vol. 87, pp. 11-20, 2020.

[3] A. F. Andreev, V. Kabanau, and V. V. Vantsevich, *Driveline systems of ground vehicles: theory and design*, 1 ed.: CRC Press, 2010.

[4] D. Savitski, V. Ivanov, K. Augsburg, T. Emmei, H. Fuse, H. Fujimoto, and L. M. Fridman, "Wheel Slip Control for the Electric Vehicle With In-Wheel Motors: Variable Structure and Sliding Mode Methods," *IEEE*

Transactions on Industrial Electronics, vol. 67, no. 10, pp. 8535-8544, 2020.

[5] D. Savitski, D. Schleinin, V. Ivanov, and K. Augsburg, “Robust Continuous Wheel Slip Control With Reference Adaptation: Application to the Brake System With Decoupled Architecture,” *IEEE Transactions on Industrial Informatics,* vol. 14, no. 9, pp. 4212-4223, 2018.

[6] B.-M. Nguyen, S. Hara, H. Fujimoto, and Y. Hori, “Slip control for IWM vehicles based on hierarchical LQR,” *Control Engineering Practice,* vol. 93, pp. 104179, 2019.

[7] K. Alipour, A. B. Robat, and B. Tarvirdizadeh, “Dynamics modeling and sliding mode control of tractor-trailer wheeled mobile robots subject to wheels slip,” *Mechanism and Machine Theory,* vol. 138, pp. 16-37, 2019.

[8] D. Tavernini, M. Metzler, P. Gruber, and A. Sorniotti, “Explicit Nonlinear Model Predictive Control for Electric Vehicle Traction Control,” *IEEE Transactions on Control Systems Technology,* vol. 27, no. 4, pp. 1438-1451, 2019.

[9] V. V. Vantsevich, "Wheel Dynamics Fundamentals for Agile Tire Slippage Modeling and Control." p. V003T01A019; 10 pages.

[10] V. V. Vantsevich, J. R. Paldan, and B. K. Farley, "Mobility Optimization and Control of a 4x4 HE-Vehicle in Curvilinear Motion on Stochastic Terrain."

[11] J. Valasek, and D. R. Downing, “An investigation of fighter aircraft agility,” 1993.

[12] J. Yi, J. Li, J. Lu, and Z. Liu, “On the Stability and Agility of Aggressive Vehicle Maneuvers: A Pendulum-Turn Maneuver Example,” *IEEE Transactions on Control Systems Technology,* vol. 20, no. 3, pp. 663-676, 2012.

[13] J. Feltman, J. Ganley, S. Hamilton, and M. Gradu, *Mechatronic torque vectoring system with enhanced controllability for augmenting the vehicle agility and safety,* 0148-7191, SAE Technical Paper, 2006.

[14] P. G. Jeremy, V. V. Vladimir, and P. Jesse, “Agile tire slippage dynamics for radical enhancement of vehicle mobility,” *Journal of Terramechanics,* vol. 65, pp. 14-37, 2016.

[15] V. V. Vantsevich, L. I. Demkiv, S. R. Klos, S. R. Misko, and L. Moradi, "An Experimental Study of Longitudinal Tire Relaxation Constants for Vehicle Traction Dynamics Modeling."

[16] M. S. Jneid, P. Harth, and P. Ficzere, “In-Wheel-Motor Electric Vehicles and Their Associated Drivetrains,” *International Journal for Traffic and Transport Engineering,* vol. 10, no. 4, 2020.

[17] V. Vantsevich, D. Gorsich, J. R. Paldan, and M. Letherwood, “A virtual driveline concept to maximize mobility performance of autonomous electric vehicles,” *SAE International Journal of Advances and Current Practices in Mobility,* vol. 2, no. 2020-01-0746, pp. 1551-1560, 2020.

[18] M. A. Salama, V. V. Vantsevich, T. R. Way, and D. J. Gorsich, “UGV with a distributed electric driveline: Controlling for maximum slip energy efficiency on stochastic terrain,” *Journal of Terramechanics,* vol. 79, pp. 41-57, 2018.

[19] J. P. Gray, V. V. Vantsevich, and J. L. Overholt, "Indices and Computational Strategy for Unmanned Ground Wheeled Vehicle Mobility Estimation and Enhancement."

[20] J. P. Gray, and V. V. Vantsevich, “Multi-vehicle convoy mobility in severe terrain conditions: Factor impact analysis, estimation and control strategy,” *Journal of Terramechanics,* vol. 61, pp. 43-61, 2015.